nature
biotechnology

Visualization of tumors and metastases in live animals with bacteria and vaccinia virus encoding light-emitting proteins

Yong A Yu[1,3], Shahrokh Shabahang[1], Tatyana M Timiryasova[2,3], Qian Zhang[3], Richard Beltz[1], Ivaylo Gentschev[4], Werner Goebel[4] & Aladar A Szalay[1,4,5]

We have shown that bacteria injected intravenously into live animals entered and replicated in solid tumors and metastases. The tumor-specific amplification process was visualized in real time using luciferase-catalyzed luminescence and green fluorescent protein fluorescence, which revealed the locations of the tumors and metastases. *Escherichia coli* and three attenuated pathogens (*Vibrio cholerae, Salmonella typhimurium*, and *Listeria monocytogenes*) all entered tumors and replicated. Similarly, the cytosolic vaccinia virus also showed tumor-specific replication, as visualized by real-time imaging. These findings indicate that neither auxotrophic mutations, nor vaccinia virus deficient for the thymidine kinase gene, nor anaerobic growth conditions were required for tumor specificity and intratumoral replication. We observed localization of tumors by light-emitting microorganisms in immunocompetent and in immunocompromised rodents with syngeneic and allogeneic tumors. Based on their 'tumor-finding' nature, bacteria and viruses may be designed to carry multiple genes for detection and treatment of cancer.

The presence of bacteria and viruses in human tumors has been recognized for more than 50 years[1]. Large numbers of bacteria[2,3] as well as viral particles have been found in tumors excised from patients[4–7].

To demonstrate the survival of bacteria in tumors, spores of the obligate anaerobe *Clostridium pasteurianum* have been injected intravenously into tumor-bearing mice and found to replicate in the hypoxic center of the tumor[8]. Intratumoral and intravenous (i.v.) injection of auxotrophic mutants of *S. typhimurium* results in elevated bacterial titers in the tumor tissues[9]. Engineered retroviral and adenoviral vectors have been administered intratumorally and systemically to tumorous animals, resulting in reduction of tumor size[10,11] and metastatic activity[10,12,13], as well as in decreased angiogenesis[13]. To determine the location of viral particles in rodents with tumors, vaccinia virus carrying the firefly luciferase expression cassette has been injected intravenously[14–17]. Subsequent luciferase assays of homogenates of excised individual organs and tumors reveal a 3- to 500-fold enhancement of light emission in tumor samples, showing the accumulation of viral particles.

To determine the spatial and temporal progression of infections in live animals with implanted tumors, tracing the movement of bacteria or virions is crucial. Isolated structural genes encoding light-emitting proteins, such as luciferases and fluorescent proteins[18–24], allow the detection of bacteria based on luciferase-catalyzed light emission or fluorescence[25–31]. Transfer of the *luxCDABE* gene cluster[32,33] into bacteria results in continuous light emission without the need of

exogenous substrate[34]. Injection of light-emitting bacteria allows the visualization and localization of bacteria in live mice[35], even through hard tissues[36]. The *Renilla reniformis* luciferase–*Aequorea victoria* green fluorescent (GFP) fusion protein (RUC-GFP)[37,38] allows real-time monitoring of gene activation in live animals based on luciferase activity and GFP fluorescence[39]. The activity of the *RUC-GFP* expression cassette inserted into vaccinia virus DNA (rVV-*RUC-GFP*) has been imaged in both virus-infected mammalian cell cultures and in virus-infected live animals[40].

In this paper, we describe the monitoring of the movement of light-emitting bacteria and vaccinia virus from the injection site to tumor tissue in live animals. We show that bacteria or vaccinia virus survived and replicated in the tumors for weeks without causing bacteremia or viremia. This was observed in both immunocompromised and immunocompetent animals with allogeneic and syngeneic tumors.

RESULTS

Clearance of bacteria and vaccinia virus from nude mice

To follow the fate of bacteria injected intravenously into the animals, we monitored each animal by low-light imaging at 2-d time intervals ($n > 10$). Injection of an attenuated *S. typhimurium*, an intracellular bacterium, immediately resulted in a disseminated light throughout the body of the animal (Fig. 1a). In contrast, injection of *V. cholerae*, an extracellular bacterium, resulted in light emission localized in the liver
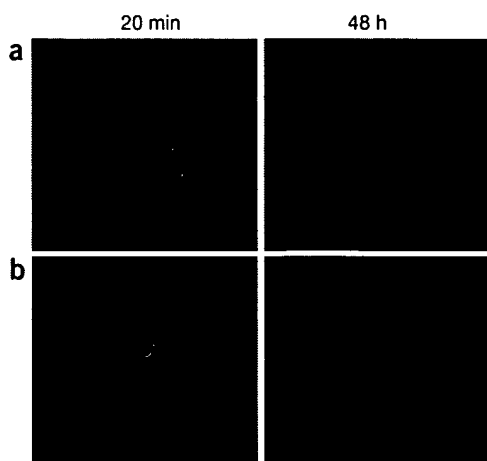
20 min   48 h

a

b

Figure 1 Visualization with the low light imager of the distribution of light-emitting bacteria injected intravenously in nude mice. (a,b) Nude mice were injected with 1×10^8 cells of attenuated *S. typhimurium* (a) and *V. cholerae* (b). Both strains were transformed with pLITE201 carrying the *luxCDABE* operon. Photon collection was for 1 min at 20 min and 48 h after bacterial injection, using the Hamamatsu ARGUS100 imaging system.

region only (Fig. 1b), as did the injection of luminescent *E. coli* (data not shown). Imaging of the same animals 24 and 48 h after injection revealed that all of the detectable light emission from the earlier time points diminished. These findings, together with the complete absence of bacteria in the blood, indicate that the light-emitting bacteria were probably eliminated by the host's immune system. The clearance was independently confirmed by the absence of light emission in all of the excised organs of the same animal (data not shown).

In addition, we examined the distribution of intravenously injected vaccinia virus in nude mice. Nu⁻/nu⁻ mice (*n* > 10) injected with rVV-*RUC-GFP* virus (1×10^8 plaque forming units (pfu)/mouse) were observed once every 3 d over a 2-week period under the low-light imager to detect luciferase-catalyzed light emission in the presence of intravenously injected coelenterazine. In parallel, the animals were also observed under a fluorescence microscope to visualize GFP expression. Two weeks after infection, neither luminescence nor green fluorescence was detected in the live animals with the exception of occasional small skin lesions. However, those minor luminescence and fluorescence signals disappeared within a week as soon as the lesions had healed. One or two weeks after viral injection, the nontumorous animals were killed. At neither time point was luminescence or green fluorescence detected in the excised brain, liver, lung, spleen, kidney or testis (data not shown), indicating that the distribution of rVV-*RUC-*

GFP virus via the blood stream did not result in significant infection of healthy organs. This was probably due to prompt clearance by the immune system.

Bacteria and vaccinia virus replicate in nude mouse tumors

To determine the localization of intravenously injected bacteria, we injected nude mice (*n* > 20) with 10-d-old implanted C6 glioma tumors (~500 mm³) in the right hind leg with 1×10^8 cells of light-emitting *S. typhimurium* or *V. cholerae*. The animals were then monitored each day for 6 d under a low light imager. The initial distribution patterns, determined immediately after injection, were similar to distributions described above (Fig. 2a(i,v)). Two days after injection, however, luminescence diminished in the entire body with the exception of the tumor region (Fig. 2a(ii,vi)). Continued monitoring of the mice at days 4 and 6 after injection showed that after an initial increase, the luminescence started to decrease in the tumors of animals injected with *S. typhimurium* (Fig. 2a(iii–iv)). Remarkably, mice injected with *V. cholerae* exhibited a dramatic increase of light emission in the tumors (Fig. 2a(vii–viii)), indicating an efficient replication of the bacteria (Table 1). The drastically different behavior of *S. typhimurium* and *V. cholerae* in tumors over time may be due to less plasmid (pLITE201) stability in *S. typhimurium*. From the results of bacterial count using homogenized tumor samples, we estimated that one week after bacterial injection, approximately 20% of the *V. cholerae* population retained the plasmid DNA, in comparison to 2% of the *S. typhimurium* population. Furthermore, intravenously injected luminescent *E. coli* DH5α (1×10^8 cells) also replicated rapidly in tumors, similar to *V. cholerae* (data not shown).

In separate experiments, nude mice (*n* > 20) with tumors approximately 500 mm³ in size were intravenously injected with rVV-*RUC-GFP* virus (1×10^8 pfu/mouse). Mice with tumors approximately 2,500 mm³ in size were then monitored for GFP fluorescence under a stereomicroscope to determine the site of viral infection and multiplication. GFP expression was first detected in the tumor region 36 h after virus injection. Unexpectedly, an intense green fluorescence was detected in a patch-like pattern exclusively in the tumor region (Fig. 2b(ii)). These patches, often located at the end of blood vessel branches, indicated that the primary site of viral replication was in cells that surround the leaky terminals of capillary vessels. Over time, the GFP signal from the center of these patches started to disappear, and new intense green fluorescent centers appeared in the form of rings at the periphery of the fading patches (data not shown). In addition to GFP, the rVV-*RUC-GFP* virus encoded a functional *R. reniformis* luciferase in the form of a fusion protein. Therefore, immediately after coelenterazine delivery by i.v. injection, a strong luciferase activity was recorded only in the tumor region (Fig. 2c(v)). By lowering the sensitivity of the low light video camera, we detected RUC expression also in localized patches mostly in the periphery of the tumor. These patch-like patterns precisely correlated with the GFP signals (data not shown). Furthermore, we also followed the infection and replication of intravenously injected rVV-*RUC-GFP* virus in the same animal for 20 d after injection (Fig. 2b(iii–v)). A continuously increasing level of GFP fluorescence and luciferase luminescence (Fig. 2c(i–iv)) was indicative of a very efficient viral replication in the tumor tissue. The tumor environment may provide a protective immunoprivileged site for viral replication subsequent to tumor entry and tumor cell

Table 1 Analyses of bacterial and viral titers from homogenized C6 glioma tumors

	Time after i.v. injection of 1×10^8 *V. cholerae*/pLITE201						
	4 h	8 h	16 h	32 h	48 h	Day 4	Day 6
Bacterial titer	3.79×10^4	3.14×10^6	1.08×10^8	5.97×10^8	6.84×10^8	8.82×10^8	1.06×10^9
(cfu/tumor)	±2.93	±2.45	±1.3	±4.26	±2.2	±2.68	±0.48
	Time after i.v. injection of 1×10^7 pfu rVV-*RUC-GFP* virus						
	36 h		Day 3		Day 5		Day 7
Viral titer (pfu/tumor)	$3.26 \times 10^6 \pm 3.86$		$7.22 \times 10^7 \pm 3.67$		$1.17 \times 10^8 \pm 0.76$		$3.77 \times 10^8 \pm 1.95$

Bacteria or viral particles were injected 13 and 7 d, respectively, after tumor cell implantation. Tumors were excised from animals (*n* = 4). I.V., intravenous. Cfu, colony-forming units. Pfu, plaque-forming units.
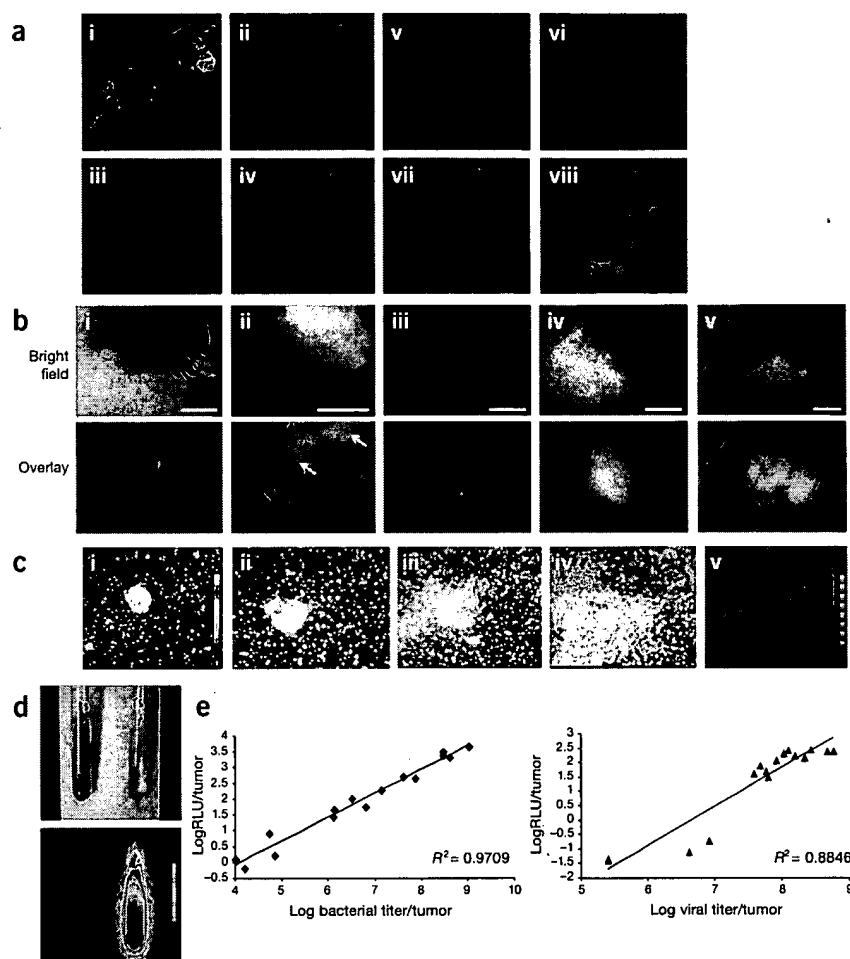
Figure 2 Intravenously injected bacteria and viruses accumulate and replicate in subcutaneous C6 rat glioma tumors in nude mice as visualized by light emission. (a) Nude mice with a C6 glioma tumor in the right hind leg were injected with 1×10^8 attenuated *S. typhimurium* (i–iv) or attenuated *V. cholerae* (v–viii) cells, both transformed with pLITE201 plasmid DNA. Photon collection was carried out for 1 min. Mice injected with *S. typhimurium* exhibited luminescence immediately through the whole animal (i). In contrast, luminescence in mice injected with *V. cholerae* was visible shortly thereafter only in the liver area (v). Two days after bacterial injection, both groups of mice demonstrated luminescence only in the tumor region (ii, vi). Light emission in the tumors infected with *S. typhimurium* slowly diminished as seen at 4 (iii) and 6 (iv) d after bacterial injection. Tumors infected with *V. cholerae* showed a marked increase in light emission 4 (vii) and 6 (viii) d after injection, suggesting continued replication of the bacteria in the tumor tissues. (b) C6 glioma cells (5×10^5) were implanted subcutaneously into the right lateral thigh. At designated days after tumor cell implantation, the animals were injected with 1×10^8 pfu of rVV-*RUC-GFP* virus particles. GFP expression was monitored under a fluorescence stereo-microscope. Bright field (top) and bright field fluorescence overlay (bottom) images of subcutaneous glioma tumor are shown. GFP signal can be observed in tumors as small as 22 mm^3 in size (i), or as old as 18 d (~2,500 mm^3 in size) (ii). In older tumors, GFP expression was seen in 'patch'-like patterns (indicated by arrows in overlay ii). Marker gene expression in the tumor of the same animal can be monitored continuously 4 (iii), 7 (iv), and 14 (v) d after i.v. viral injection. Scale bars = 5 mm. (c) Real-time, low-light images of tumors at different time points (36 h (i), 3 d (ii), 5 d (iii) and 7 d (iv)) after i.v. injection of 1×10^7 of rVV-*RUC-GFP* indicate the location of RUC-triggered light emission in the presence of i.v. injected coelenterazine (2.5 μg ethanol solution) in anesthetized nude mice. Panel v shows the low light and bright field overlay image to indicate the tumor-specific luminescence signal. (d) Analysis of the presence of bacteria in blood and tumor fluid samples in overnight culture in Luria Broth medium. Blood and tumor fluid samples were taken from a nude mouse carrying a subcutaneous C6 glioma tumor 1 week after i.v. injection of 1×10^8 light-emitting *V. cholerae*. Fifty microliters of tumor fluid was withdrawn by inserting a 29½ gauge needle directly into the center of the tumor. Only the tumor fluid was shown to be positive for light-emitting bacteria (right tube), whereas no bacteria were detected in the blood (left tube). (e) Correlation of luciferase activities with bacterial or viral titers in tumors. Seven or 13 days after C6 glioma cell implantation, nude mice were injected with either 1×10^8 of *V. cholerae*/pLITE201 or with 1×10^7 pfu of rVV-*RUC-GFP*, respectively. At different time points after infection (as shown in **Table 1**), mice were killed. The tumors were excised, homogenized and assayed for bacterial (left) and viral (right) titers. The bacterial luciferase and *Renilla* luciferase activities (reported as relative light units (RLU)) in the tumor homogenates were measured using a luminometer.

infection. The viral replication in the tumor tissues was also independently confirmed by determination of the viral titers in excised tumors (Table 1) and organs obtained at various time points. Homogenates of C6 glioma tumors 1,500 mm^3 in size yielded 2–5×10^8 plaques in comparison to homogenates of the entire liver or spleen, which yielded less than 2,600 or 100 plaques, respectively, 7 d after injection of 1×10^7 pfu of rVV-*RUC-GFP*. In addition, the luciferase assay using tumor homogenates showed direct correlation between viral titer and luciferase-based light emission (Fig. 2e, right).

The sites of viral infection were determined in exposed tumors, where the GFP fluorescence was found to be concentrated exclusively in the tumor tissue (Fig. 3). Neither the skin nor the nontumorous thigh muscles showed fluorescence. In contrast, cross sections of the tumor revealed strong green fluorescent regions organized as patches

in the periphery of the tumor (arrows in Fig. 3b(iii)), indicating the sites where the vaccinia virus–directed gene expression was most active. Analysis of tissue sections under a fluorescence microscope revealed that GFP fluorescence was present in large clusters of cells within the tumor (Fig. 3a). However, no fluorescence was visible in nontumorous tissues.

To determine whether the tumor size and the degree of vascularization affect bacterial entry and colonization, we injected animals with 0-, 2-, 4-, 6-, 8- and 10-d-old subcutaneous glioma tumors with attenuated *S. typhimurium* and *V. cholerae* containing the pLITE201 plasmid DNA. The earliest glioma tumor age at which luminescence was observed was day 8 with a tumor volume of approximately 200 mm^3. When injected intravenously with rVV-*RUC-GFP* virus, nude mice exhibited tumor-specific viral replication 6 d after implantation of
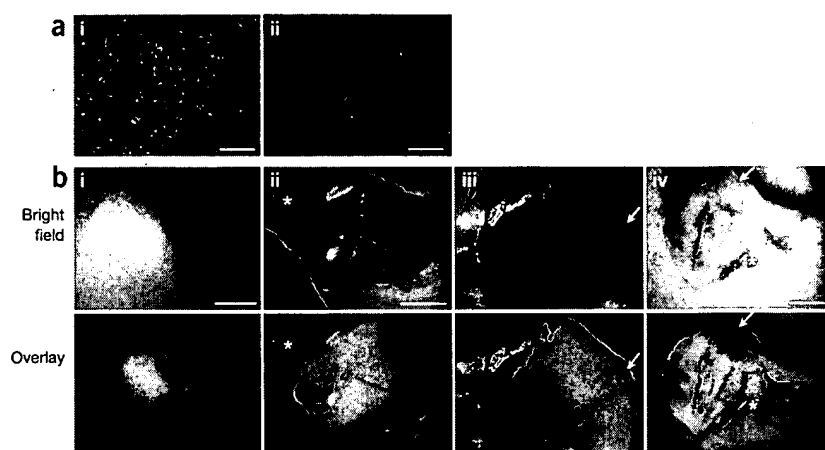
Figure 3 Localization of bacterial colonization and viral infection in subcutaneous C6 glioma tumors. (a) Bright field (i) and fluorescence (ii) images of tumor cells expressing GFP. Frozen sections (30 μm thick) of the glioma tumor tissues were prepared from a nude mouse that has been injected with 1×10^8 pfu of rVV-*RUC-GFP* virus. Scale bars = 50 μm. (b) Five days after the subcutaneous implantation of 5×10^5 C6 glioma cells into the right lateral thigh, 1×10^8 pfu of rVV-*RUC-GFP* virus were injected intravenously. Five days after viral injection, the animal was anesthetized and killed for analysis of GFP expression under fluorescence microscope. The tumor was visualized externally (i), with the overlying skin reflected (ii), in cross section (iii) and in the amputated leg (iv). The strongest GFP expressions are seen as patches located along the outer surface of the tumor on the right (arrows in iii). Sharp difference of GFP expression in tumor tissue and in the normal muscle tissue (arrows in iv) is clearly visible. The reflected skin is marked with asterisks (ii, iv). Scale bars = 5 mm.

C6 glioma cells, as determined by GFP expression 5 d after viral injection in a tumor volume of ~22 mm³ (Fig. 2b(i)).

Additionally, nude mice bearing subcutaneous PC-3 human prostate tumors were intravenously injected with the attenuated *L. monocytogenes* (1×10^7) transformed with p*SOD-GFP* plasmid DNA. Nearly 27 h after bacterial injection, a weak GFP signal originating from the tumor region was already detectable (Fig. 4a(i)), and no GFP signal was registered elsewhere in the animal. To examine whether the intravenously injected vaccinia virus was able to enter, infect and replicate in tumors other than gliomas, we introduced rVV-*RUC-GFP* into mice with implanted subcutaneous PC-3 human prostate carcinoma. Although the PC-3 implants from which tumors developed grew at a much slower rate than the subcutaneous glioma tumors, these tumors showed the same tumor-specific replication of vaccinia virus (Fig. 4a(ii)). GFP expression was initially detected 3 d after virus injection, and the intense fluorescence lasted throughout the 3-week observation period.

In addition, we also tested the HT1080 human fibrosarcoma cell line, which was stably transformed with a *GFP* expression cassette, and therefore the boundary of the tumors formed by this cell line can be clearly defined on the surface of live animals by fluorescence microscopy. Intravenous injection of *V. cholerae* or *S. typhimurium* (1×10^8) into nude mice carrying such subcutaneous HT1080 fibrosarcoma tumors resulted in tumor-specific colonization by bacteria, and the luminescent signal was seen only within the boundary of the fluorescent tumor (data not shown).

Bacteria and virus replicate in C57 mouse tumors

Immunocompetent C57 mice ($n = 2$) bearing orthotopic MB-49 murine bladder tumors were injected intravenously with attenuated *V. cholerae*. Bacterial light emission was noted in the bladder region of live animals (Fig. 4b(i)). After abdominal incision, the bladder was

exposed, and the light emission was located in the bladder region (Fig. 4b(ii)). Upon surgical removal of the bladder from the mouse, it continued to glow while the rest of the animal body was dark (Fig. 4b(iii–iv)). This experiment showed that even small bladder tumors (<20 mm³ in size) had the propensity to retain bacteria from the bloodstream in immunocompetent mice. C57 mice with MB-49 tumors were also intravenously injected with rVV-*RUC-GFP*, and 5 d after virus injection, GFP expression was observed only in the bladder tumor region (Fig. 4c).

When Lewis rats with intracranial C6 glioma tumor in the brain were injected intravenously with attenuated *V. cholerae* (1×10^9), low levels of luminescence activity were observed through the skull. Visualization of the excised brain under the imager revealed strong luminescence at the site of the tumor (Fig. 4d(i)). However, control rats injected with phosphate-buffered saline (PBS) alone showed no luminescence. Similarly, weak GFP fluorescence was observed in the surgically exposed intracranial glioma tumors 5 d after i.v. injection of rVV-*RUC-GFP* virus into rats (Fig. 4d(ii–iii)). Taken together, these data show that both bacteria and vaccinia virus did enter and replicate in brain gliomas similarly to the way they replicated in the other tumor models described above.

Bacteria and vaccinia virus reveal the location of metastases

Female nude mice ($n = 4$) bearing 6-month-old MCF-7 human metastatic mammary carcinoma tumors transformed with pro-insulin-like growth factor (IGF)-II expression cassette[41] (~400–500 mm³) in the right breast pad were injected intravenously with cells of *V. cholerae*. Two days after injection, the breast tumor was colonized by the bacteria (Fig. 5a(ii)), whereas the liver region became silent (Fig. 5a(i–ii)). Light emission was also visible in the left breast (metastases, ~36 mm³), indicating the presence of bacteria (Fig. 5a(ii)). Both tumors remained luminescent after 5 d (Fig. 5a(iii)), and strong luminescence activity continued for over 45 d in the primary tumor (data not shown), during which time the mice remained healthy. Experiments using luminescent *E. coli* also showed efficient replication in breast tumors (Fig. 5a(v–vi)).

Female nude mice ($n = 4$) with established MCF-7 human breast tumors (~400–500 mm³) were intravenously injected with rVV-*RUC-GFP* virus. A strong GFP expression was observed in the breast tumor region 6 d after virus injection (Fig. 5b(i–ii)). Visualization of cross sections of virus-infected breast tumors revealed fluorescent 'islands' throughout the tumors, with no indication of central or peripheral preference of infection (Fig. 5b(iii)). A smaller metastasized tumor at the left side of the chest also showed intense GFP fluorescence (Fig. 5b (iv–vi)). Metastasized tumor nodules as small as 0.5 mm in diameter on the surface of the excised lung were also positive for GFP fluorescence (Fig. 5b(vii)). The presence of a strong RUC-mediated light emission confirmed the expression of the RUC-GFP fusion protein in these breast tumors, but nowhere else in the body (data not shown). These experiments demonstrate that intravenously delivered VV particles, after entering the tumors and metastases, replicated in the tumor tissue, thereby revealing the location of tumors and metastases.
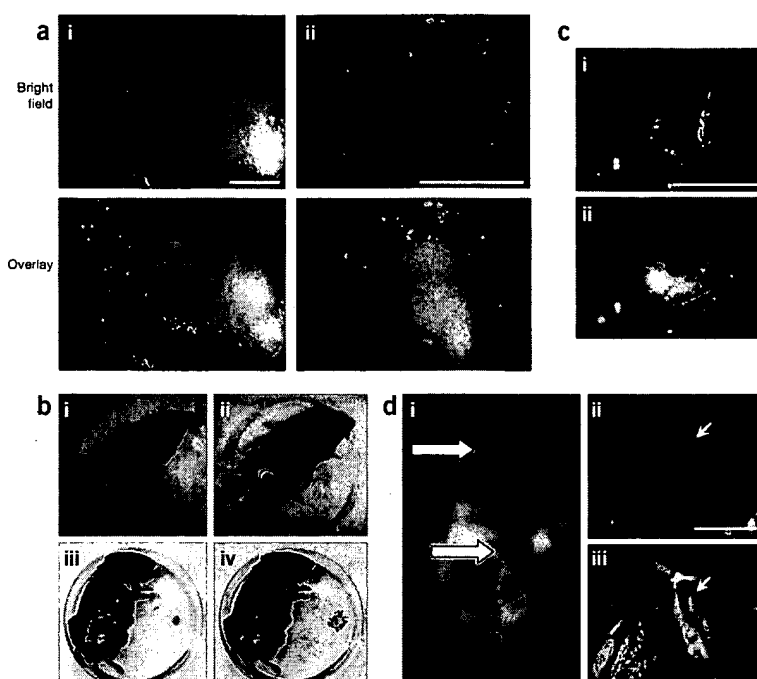
Figure 4 Bacterial and vaccinia virus show tumor-specific localization in different tumorous mice models. (**a**) Intravenously injected *L. monocytogenes* and vaccinia virus accumulate and replicate in subcutaneous PC-3 human prostate tumors in nude mice. (**i**) Mice were injected with 1 × 10⁸ of attenuated *L. monocytogenes* cells transformed with p*SOD-GFP* plasmid DNA carrying the *GFP*-cDNA expression cassette. GFP fluorescence was observed under a fluorescence stereomicroscope. Twenty-seven hours after the injection, GFP signal was detected only in the tumor region. (**ii**) One week after i.v. injection of r*VV-RUC-GFP* at 1 × 10⁸ pfu/mouse, GFP expression was specifically localized to the PC-3 tumors in nude mice. (**b–d**) Bacteria and vaccinia virus show tumor-specific localization in immunocompetent rodents. C57 mice were injected intravenously either with 1 × 10⁸ attenuated *V. cholerae* cells transformed with pLITE201 carrying the *lux* operon (**b**) or with 1 × 10⁸ pfu/mouse of r*VV-RUC-GFP* (**c**). Nine days after delivery of the bacteria, luminescence was noted in the bladder region of the whole animal (**b(i)**). The animal was killed and an abdominal incision was made to expose the bladder. Light emission was limited to the bladder region (**b(ii)**). After removal of the bladder (**b(ii)**) from the mouse, the entire source of light emission was removed (**b(iv)**), as shown by the overlay of the low light photon emission image on the photographic image of the excised bladder. Similarly, 9 d after the delivery of virus, green fluorescence was noted in the surgically exposed bladder tumors (**c(ii)**). (**d**) Lewis rats were injected intravenously either with 1 × 10⁹ attenuated *V. cholerae* cells transformed with pLITE201 (**i**) or with 1 × 10⁸ pfu of r*VV-RUC-GFP* (**ii–iii**). Twenty-four hours after injection of the bacteria, faint luminescence was noted in the head region of the whole animal. The animals were killed. Photon collection from excised tumorous brain was carried out for 1 min, and strong luminescence was confirmed in the tumor region of tumor-bearing brain (**i**, marked with arrows). Similarly, 5 d after viral injection, weak GFP expression was noted in the surgically exposed intracranial tumors in rats (**iii**). Bright field (**c(i)**, **d(ii)**), and bright field/fluorescence overlay (**c(ii)**, **d(iii)**) images are shown. Scale bars = 5 mm.

Do bacteria and vaccinia virus reenter the blood circulation?

To examine whether bacteria are released from tumors, reenter the blood circulation and colonize newly implanted tumors, a second tumor (subcutaneous C6 glioma) was developed on the right hind leg of animals already carrying a strong light-emitting breast tumor. Continuous monitoring of such animals showed no light emission in the second tumor implant, showing that bacteria from the original breast tumor were either not released or were not released in sufficient numbers to be able to colonize the second tumor. However, a repeated i.v. injection of 1 × 10⁸ cells of attenuated *V. cholerae* into the same animal showed strong luminescence activity in the newly implanted tumor concomitantly with continuous light emission from the original

tumor. Samples of blood and tumor fluid from subcutaneous C6 glioma tumors colonized by light-emitting *V. cholerae* were collected. Analyses of the blood samples showed complete absence of *V. cholerae*, whereas the tumor samples contained large numbers of luminescent bacteria (**Fig. 2d**). To determine the level of viral particles released from breast tumors infected with r*VV-RUC-GFP* virus, we implanted C6 glioma cells into the thigh of these mice. No GFP signal was detected in the newly formed glioma tumor, indicating that no viral replication occurred in this tumor. However, both glioma and breast tumors showed strong fluorescence after a repeated i.v. injection of r*VV-RUC-GFP* virus. Based on these findings, we conclude that the release of bacteria and vaccinia virus from infected tumors into blood either did not occur or the released number of microorganisms was insufficient to colonize the newly implanted tumors. The limited release of bacteria or virus from tumors should provide greater safety for bacterium- or virus-mediated detection and therapy of tumors.

DISCUSSION

We show here that bacteria and vaccinia virus gained entry and replicated only in the tumor tissue. Localization of the light-emitting microorganisms in live animals could be followed in real time through low light and fluorescence imaging. Three attenuated bacterial strains, *V. cholerae*, *S. typhimurium* and *L. monocytogenes*, were found to enter and replicate in tumors. Similarly, *E. coli* DH5α also showed tumor-specific localization. In contrast to a previous report[9], no mutations affecting the survival of the bacteria were required for tumor-specific entry and replication of bacteria. We also demonstrated that both primary and metastasized tumors could be visualized using the labeled bacteria. Furthermore, our experiments showed that intravenously injected light-emitting bacteria colonized intracranial tumors in immunocompetent rats and bladder tumors in immunocompetent mice, implying that the tumor microenvironment is an immune privileged site, which provides protection against the host immune system.

Minutes after i.v. injection, the bacteria were distributed throughout the entire animal, and then concentrated in the spleen and the liver as a result of macrophage surveillance. Light emission by bacteria that escaped immune surveillance by entering into the tumor was barely detectable immediately after injection. Owing to rapid bacterial replication, light emission originating from the bacteria within tumors became easily detectable *in vivo*. Visualization experiments using animals carrying breast tumors demonstrated that three sites, namely, the incision wound, the primary tumor and the metastatic tumor were first colonized by the bacteria. One week later, the wound sites became nonluminescent, probably after reconnecting the vasculature with the
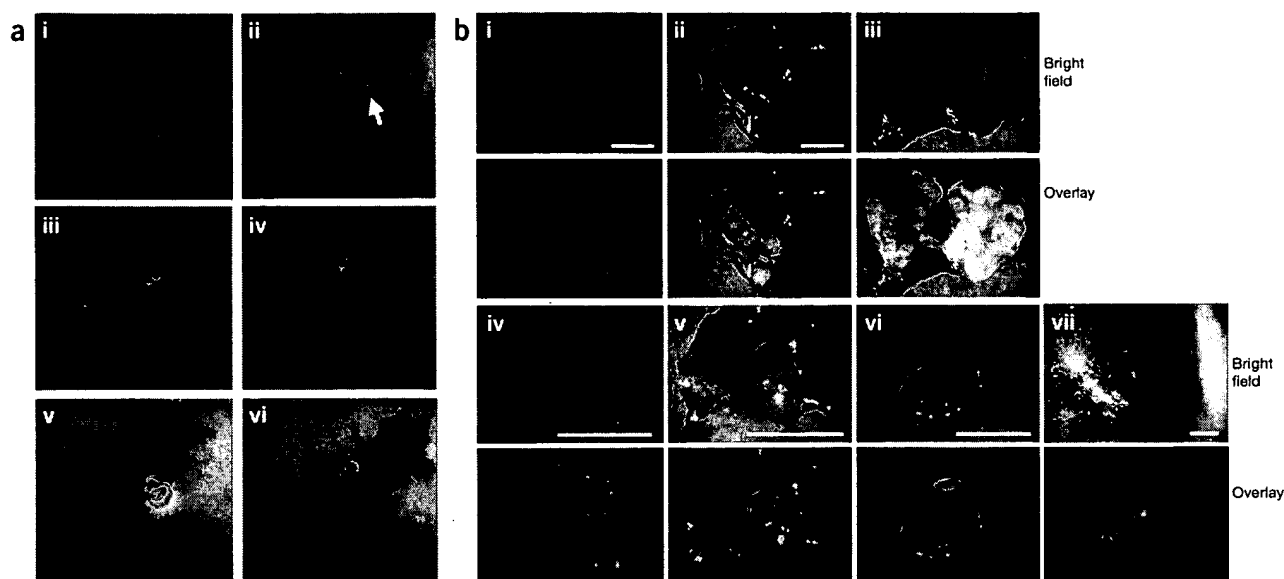
Figure 5 Intravenously delivered light-emitting bacteria and recombinant vaccinia virus mark the location of primary breast tumors and their metastases in nude mice. (a) Nude mice with breast tumors in the right breast pad were injected intravenously with 1×10^8 attenuated *V. cholerae* (i–iv) or with 1×10^8 *E. coli* (v–vi) cells transformed with pLITE201 plasmid DNA. Photon collection was carried out for 1 min. Twenty minutes after bacterial delivery, luminescent *V. cholerae* were observed in the liver (i). Forty-eight hours after injection, light emission was noted in the primary breast tumor located in the right breast area, in a metastatic tumor (arrow) in the left breast area and in the femoral vein incision wound (ii). At 5 d, the light emission was visible only in the tumor regions; there was none in the wound (iii). Eight days after injection of bacteria, the luminescent activity was no longer detectable in the metastatic tumor region but remained strong in the primary breast tumor (iv). Specific localization of *E. coli* for breast tumors in nude mice was also observed 2 d after i.v. injection of bacteria (v, side view; vi, ventral view). (b) Nude mouse carrying breast tumor was injected intravenously with 1×10^8 pfu of rVV-*RUC-GFP* virus. Both the primary tumor (i–iii) and the metastasized tumor (iv–vi) were visualized externally (i,iv), with overlying skin removed (ii,v), and when they were split open (iii,vi). GFP expression in lung metastases in the same animal was also visualized (vii). Scale bars = 5 mm (i–vi), and 1mm (vii).

lymphatic system and restoring the immune surveillance. However, presumably because of an impaired lymphatic system[42], the removal of bacteria from the primary tumor could not occur and therefore continuous light emission was observed over 45 d after injection. This observation showed that only an established tumor possessed the ability to protect bacteria from immune clearance. Therefore, the degree of tumor vascularization and the status of tumor lymphangiogenesis may be the determining factors for tumor colonization by bacteria. The size of different solid tumors did not appear to determine their capability to protect bacteria from the immune system. For example, the minimal size of subcutaneous glioma tumor that was colonized by *V. cholerae* was ~200 mm³, whereas the bladder tumors (~20 mm³) in C57 mice were colonized with similar intensity.

Early observations that strains of *Clostridia* preferentially proliferate in necrotic centers of tumors[43] lead to the hypothesis that, unlike normal tissues, the hypoxic environment in tumors provides anaerobic growth conditions[8,44], as it may do for the growth of anaerobic *Bifidobacterium longum*[45]. However, auxotroph mutants of *S. typhimurium* have been shown to multiply in tumors in mice, as found after analysis of homogenized tissues[9,46]. Therefore, anaerobicity in the necrotic center of the tumor alone is not the factor that determines bacterial accumulation in the tumor. In contrast, based on our data, we propose that the entry, survival and replication of bacteria in tumors is dependent on tumor vascularization and tumor immune microenvironment, which provides a sanctuary for a small number of bacteria that will escape clearance by the immune system.

Simultaneously, we also found that intravenously injected vaccinia virus was preferentially localized in different tumors in live animals.

Tumor-specific replication by vaccinia virus was demonstrated in subcutaneous C6 glioma and PC-3 tumors, MCF-7 tumors in nude mice, and orthotopic MB-49 tumors in C57 mice. Viral DNA-coded green fluorescence was detected at the site of injection as early as 2 d after injection in contrast to data reported previously[47,48]. Accumulation and replication of vaccinia virus were observed in real time in tumors ranging from 22 to 2,500 mm³ in volume. Therefore, the unique tumor microenvironment and tumor cell properties, rather than the size of the tumor, seem to determine the entry and survival of viral particles in tumor tissues. These findings are very similar to those found with bacteria. Interestingly, combined i.v. injection of bacteria and vaccinia virus into the same tumor-bearing animal resulted in both bacterial and viral accumulation and replication in the same tumor.

In addition to the visualization of primary tumors, the bacteria and viral particles are also naturally capable of finding small metastatic nodules. Tumor-like nodules as small as 0.5 mm³ were detected on the surface of the lungs of tumor-bearing mice based on GFP fluorescence after surgical exposure. Since metastatic lesions of small size are difficult to detect, the vaccinia virus–mediated, tumor-specific targeting system may become a clinical tool for sensitive detection and removal of secondary tumors, as well as primary tumors at an early stage.

The results of our experiments demonstrate that the recombinant rVV-*RUC-GFP* of Lister-Institute for Viral Preparations (LIVP) strain replicated specifically in tumorous and in inflamed tissues. Therefore, the tumor-specific infection and replication of vaccinia virus may not be dependent on the availability of metabolites provided by actively dividing cells as suggested by researchers[17], who used a thymidine

kinase gene–deleted mutant strain of vaccinia virus. Preferential infection of tumor tissues by vaccinia virus and its survival and replication may be the result of fundamental structure and immunological differences between nontumorous and tumorous tissues. Vaccinia virus injected into the bloodstream may enter the tumors through capillaries and replicate in a tumor environment lacking immune protection. In contrast, the rest of circulating viral particles are cleared by the host's immune system shortly after i.v. delivery.

In this study, we demonstrated the real-time visualization of localization, survival and replication of engineered bacteria and vaccinia virus in implanted tumors and their metastases in live animals. We propose that a small number of blood-borne microorganisms may enter tumors through leaky vasculature, thereby escaping the host's immunosurveillance and finding sanctuary in the tumor tissues. These systems may be applied to the detection of tumors and metastases and may allow the development of tumor-specific gene therapy protocols.

METHODS

Bacterial and viral strains. The bacterial strains used were E. coli (DH5α), attenuated S. typhimurium (SL7207 hisG46, DEL407[aroA544:Tn10]) and attenuated V. cholerae (Bengal 2 Serotyp O139, M010 DattRS1). The plasmid pLITE201 (obtained from F. Marincs[49]), containing luxCDABE, was used to transform E. coli, S. typhimurium and V. cholerae to produce light-emitting bacterial strains. The plasmid pSOD-GFP, carrying the GFP gene construct under the control of the SOD promoter, was used to transform L. monocytogenes.

The viral strain used in this study was LIVP vaccine strain of vaccinia virus. Recombinant vaccinia virus rVV-RUC-GFP was constructed by inserting via homologous recombination the RUC-GFP cassette[39], which contains the RUC and GFP cDNA sequences under the control of a synthetic early/late promoter of vaccinia, into the nonessential region of the vaccinia virus genome[40]. The rVV-RUC-GFP virus was propagated in CV-1 African green monkey kidney fibroblast cells and purified by centrifugation through a sucrose gradient. The titer of rVV-RUC-GFP virus was determined by plaque assay on CV-1 cells and expressed as pfu/ml.

Tumor cell lines. The C6 rat nitrosourea-induced glioma cell line (ATCC) was cultured in RPMI-1640 medium (Cellgro, Mediatech) supplemented with 10% FBS, 100 units/ml penicillin G, 250 ng/ml amphotericin B, and 100 units/ml streptomycin (1×). The PC-3 human prostate carcinoma cell line (ATCC), MB-49 murine bladder carcinoma cells, HT1080 human fibrosarcoma cells transformed with retrovirus carrying the GFP expression cassette (pLEIN, Clontech), and CV-1 cells were cultured in DMEM (Cellgro, Mediatech) supplemented with 10% FBS and 1× penicillin/amphotericin/streptomycin. The MCF-7 human mammary carcinoma cell line (ATCC), permanently transformed with a plasmid carrying pro-IGF-II cDNA (a gift from Daisy deLeon), was cultured in DMEM/F12 medium supplemented with 5% FBS and 560 µg/ml of G418 (Life Technologies).

Recipient animals and tumor models. Five- to six-week-old male BALB/c athymic nu⁻/nu⁻ mice (25–30 g body weight) and Lewis rats (250–300 g) were purchased from Harlan. To generate nude mice carrying subcutaneous glioma tumors, C6 glioma cells were harvested and the number of viable cells was determined by the trypan blue exclusion method. Then 5×10^5 viable cells in 100 µl of PBS were injected subcutaneously into the right lateral thigh of each mouse. Tumor growth was monitored by recording size with a digital caliper. Tumor volume (mm³) was estimated by the formula (L × H × W)/2, where L is the length, W is the width and H is the height of the tumor in millimeters. Mice bearing subcutaneous prostate tumors and subcutaneous colon fibrosarcoma were generated over a period of 1 month after subcutaneous implantation of 3×10^6 PC-3 human prostate cells or 5×10^5 retrovirus-transformed HT1080 fibrosarcoma cells, respectively.

Intracerebral glioma tumors were generated by injecting C6 glioma cells into the brain of rats. Rats were anesthetized with sodium pentobarbital (Nembutal sodium solution, Abbot Laboratories; 60 mg/kg body weight). A midline scalp incision (0.5–1 cm) was made, skin was reflected and a 1 mm burr hole was made in the skull located 2 mm to the left and 2.5 mm posterior to the bregma.

Tumor cells were pipetted into an insulin syringe fitted with a 29½-gauge needle and mounted in a stereotactic holder. The needle was inserted vertically through the burr hole to a depth of 3 mm. After injection into the brain of a 10 µl volume of either 5×10^5 C6 cells or PBS as control, the needle was kept in place for 15 sec and then withdrawn. The skin incision was closed with surgical clips.

To generate the MCF-7 breast tumor animal model, 4–6-week-old female nude mice were first implanted with 17β-estradiol pellets (0.72 mg per pellet, 90-d release; Innovative Research of America) in the dorsal skin to facilitate breast tumor development and metastasis. One day after estrogen pellet implantation, 1×10^6 MCF-7 human breast carcinoma cells transformed with pro-IGF-II were injected directly into the second left mammary fat pad of each mouse through an incision just below the second nipple. For orthotopic transplants, tumors developed from implanted cells were resected and minced into 1-mm³ cubes for tissue transplantation into the mammary fat pad. Solid tumor metastases as large as 50 mm³ may appear in other mammary fat pads 3–6 months after cellular implantation. Extensive lung metastases may also occur within 3–6 months after cellular implantation. C57 mice with an implanted MB-49 murine tumor in the bladder were generated by M. Lilly and kindly provided by I. Fodor.

All animal experiments were carried out in accordance with protocols approved by the Loma Linda University animal research committee and by the Institutional Animal Care and Use Committee (IACUC) of LAB Research International located in San Diego Science Center. Anesthesia of animals was carried out using Nembutal (60 mg/kg body weight). The animals containing recombinant DNA materials and attenuated pathogens were kept in the animal care facilities in Loma Linda University or in LAB Research International at biosafety level two.

I.V. injection of bacteria or vaccinia virus into animals. Unless specified otherwise, 1×10^8 light-emitting bacteria or 1×10^8 pfu of purified rVV-RUC-GFP virus, both suspended in 100 µl of PBS, were injected intravenously with a 1-cc insulin syringe equipped with a 29¹/₂-gauge needle through the surgically exposed femoral vein. After the injections, the incisions were sutured.

Histology of tumors. Under anesthesia, the animals were killed with Nembutal. The tissues were removed, embedded in Tissue-Tek OCT compound (Miles Scientific) and immediately frozen in liquid nitrogen. Frozen sections (30–60 µm in thickness) were cut using a Reichert-Jung Cryocut 1800 cryostat at –20 °C. GFP fluorescence of the tissues was monitored under a Leica fluorescence microscope and the images were recorded using Photoshop software.

Detection of luminescence and fluorescence. To analyze bacterial luciferase activity, anesthetized animals were placed inside the dark box for photon counting (ARGUS 100 Low Light Imager, Hamamatsu). Photon collection was for 1 min from ventral and dorsal views of the animals, and the images were recorded using Image Pro Plus 3.1 software (Media Cybernetics). A light image was also recorded, which was then superimposed upon the low light image to localize the luminescence activity. RUC activities were determined in anesthetized animals after i.v. injection of a mixture of 5 µl of coelenterazine (0.5 µg/µl diluted ethanol solution) and 95 µl of luciferase assay buffer (0.5 M NaCl; 1 mM EDTA; and 0.1 M potassium phosphate, pH 7.4). Animals were then imaged under the low light imager similarly to imaging animals with bacterial luciferase activities. Luciferase activities in excised and grounded organs were measured using a Turner TD-20e luminometer. Imaging of GFP expression in tumors of live animals was performed using a Leica MZ8 stereo fluorescence microscope equipped with a mercury lamp power supply and a GFP filter (excitation at 470 nm). Images were captured using a SONY DKC-5000 3CCD digital photo camera.

ARTICLES

1. Abelmann, H.W. in *Cancer as I See It* (Philosophical Library, Inc., New York, 1951).
2. Llinares, P. *et al.* Infected atrial myxoma simulating infective endocarditis. *Enferm. Infecc. Microbiol. Clin.* **11**, 378–381 (1993).
3. Liao, W.Y. *et al.* Bacteriology of infected cavitating lung tumor. *Am. J. Respir. Crit. Care Med.* **161**, 1750–1753 (2000).
4. Di Virgilio, G., Lavenda, N. & Siegel, D. Viral particles in human breast cancer. *Oncologia* **19**, 341–348 (1965).
5. Williamson, A.L., Jaskiesicz, K. & Gunning, A. The detection of human papillomavirus in oesophageal lesions. *Anticancer Res.* **11**, 263–265 (1991).
6. Liu, B. *et al.* Identification of a proviral structure in human breast cancer. *Cancer Res.* **61**, 1754–1759 (2001).
7. Chang, F., Syrjanen, S., Shen, Q., Wang, L. & Syrjanen, K. Screening for human papillomavirus infections in esophageal squamous cell carcinomas by *in situ* hybridization. *Cancer* **72**, 2525–2530 (1993).
8. Lemmon, M.J. *et al.* Anaerobic bacteria as a gene delivery system that is controlled by the tumor microenvironment. *Gene Ther.* **4**, 791–796 (1997).
9. Pawelek, J.M., Low, K.B., & Bermudes, D. Tumor-targeted *Salmonella* as a novel anti-cancer vector. *Cancer Res.* **57**, 4537–4544 (1997).
10. Sauter, B.V., Martinet, O., Zhang, W., Mandeli, J. & Woo, S.L.C. Adenovirus-mediated gene transfer of endostatin *in vivo* results in high level of transgene expression and inhibition of tumor growth and metastases. *Proc. Natl. Acad. Sci. USA* **97**, 4802–4807 (2000).
11. Gordon, E.M. *et al.* Systemic administration of a matrix-targeted retroviral vector is efficacious for cancer gene therapy in mice. *Hum. Gene Ther.* **12**, 193–204 (2001).
12. Block, A. *et al.* Gene therapy of metastatic colon carcinoma: regression of multiple hepatic metastases by adenoviral expression of bacterial cytosine deaminase. *Cancer Gene Ther.* **7**, 438–445 (2000).
13. Chen, C.T. *et al.* Antiangiogenic gene therapy for cancer via systemic administration of adenoviral vectors expressing secretable endostatin. *Hum. Gene Ther.* **11**, 1983–1996 (2000).
14. Gnant, M.F.X. *et al.* Tumor-specific gene delivery using recombinant vaccinia virus in a rabbit model of liver metastases. *J. Natl. Cancer Inst.* **91**, 1744–1750 (1999).
15. Gnant, M.F., Puhlmann, M., Bartlett, D.L. & Alexander, H.R. Jr. Regional versus systemic delivery of recombinant vaccinia virus as suicide gene therapy for murine liver metastases. *Ann. Surg.* **230**, 352–360 (1999).
16. McCart, J.A. *et al.* Complex interactions between the replicating oncolytic effect and the enzyme/prodrug effect of vaccinia-mediated tumor regression. *Gene Ther.* **7**, 1217–1223 (2000).
17. Puhlmann, M. *et al.* Vaccinia as a vector for tumor-directed gene therapy: biodistribution of a thymidine kinase-deleted mutant. *Cancer Gene Ther.* **7**, 66–73 (2000).
18. Belas, R. *et al.* Bacterial bioluminescence: isolation and expression of the luciferase genes from *Vibrio harveyi*. *Science* **218**, 791–793 (1982).
19. De Wet, J.R., Wood, K.V., Deluca, M., Helinski, D.R. & Subramani, S. Firefly luciferase gene: structure and expression in mammalian cells. *Mol. Cell. Biol.* **7**, 725–737 (1987).
20. Prasher, D.C., McCann, R.O., Longiaru, M. & Cormier, M.J. Sequence comparisons of complementary DNAs encoding aequorin isotypes. *Biochem.* **26**, 1326–1332 (1987).
21. Foran, D.R. & Brown, W.M. Nucleotide sequence of the *LuxA* and *LuxB* genes of the bioluminescent marine bacterium *Vibrio fischeri*. *Nucleic Acids Res.* **16**, 777 (1988).
22. Escher, A., O'Kane, D.J., Lee, J., & Szalay, A.A. Bacterial luciferase αβ fusion protein is fully active as a monomer and highly sensitive *in vivo* to elevated temperature. *Proc. Natl. Acad. Sci. USA* **86**, 6528–6532 (1989).
23. Lorenz, W.W., McCann, R.O., Longiaru, M. & Cormier, M.J. Isolation and expression of a cDNA encoding *Renilla reniformis* luciferase. *Proc. Natl. Acad. Sci. USA* **88**, 4438–4442 (1991).
24. Prasher, D.C., Eckenrode, V.K., Ward, W.W., Prendergast, F.G. & Cormier, M.J. Primary structure of the *Aequorea victoria* green-fluorescent protein. *Gene* **111**, 229–233 (1992).
25. Engebrecht, J., Simon, M. & Silverman, M. Measuring gene expression with light.

26. Legocki, R.P., Legocki, M., Baldwin, T.O. & Szalay, A.A. Bioluminescence in soybean root nodules: demonstration of a general approach to assay gene expression *in vivo* using bacterial luciferase. *Proc. Natl. Acad. Sci. USA* **83**, 9080–9084 (1986).
27. Chalfie, M., Tu, Y., Euskirchen, G., Ward, W.W. & Prasher, D.C. Green fluorescent protein as a marker for gene expression. *Science* **263**, 802–805 (1994).
28. Langridge, W.H.R. *et al.* A luciferase marker gene system to monitor gene expression in bacteria, plant and virus infected animal cells. *Proceedings of the VIIth Int. Symp. on Bio & Chemiluminescence, Banff, Canada, March 14–18, 1993* (eds. Szalay, A.A. *et al.*) 222–226 (Wiley, Chichester, UK, 1993).
29. O'Kane, D.J. *et al.* Visualization of bioluminescence as a marker of gene expression in *Rhizobium*-infected soybean root nodules. *J. Plant Mol. Biol.* **10**, 387–399 (1988).
30. Wang, G., Mayerhofer, R., Langridge, W.H.R., & Szalay, A.A. in *Proceedings of the VIIth Int. Symp. on Bio & Chemiluminescence, Banff, Canada, March 14–18, 1993* (eds. Szalay, A.A. *et al.*) 232–238 (Wiley, Chichester, UK, 1993).
31. Giacomin, L.T. & Szalay, A.A. Expression of a *PALI* promoter luciferase gene fusion in *Arabidopsis thaliana* in response to infection by phytopathogenic bacteria. *Plant Sci.* **116**, 59–72 (1996).
32. Lee, C.Y., Szittner, R. & Meighen, E.A. The *lux* genes of the luminous bacterial symbiont, *Photobacterium leiognathi*, of the ponyfish. Nucleotide sequence, difference in gene organization and high expression in mutant *Escherichia coli*. *Eur. J. Biochem.* **201**, 161–167 (1991).
33. Meighen, E.A. & Szittner, R. Multiple repetitive elements organization of the *lux* operons of luminescent terrestrial bacteria. *J. Bacteriol.* **174**, 5371–5381 (1992).
34. Fernandez-Pinas, F. & Wolk, C.P. Expression of *luxCD-E* in *Anabaena sp.* can replace the use of exogenous aldehyde for *in vivo* localization of transcription by *luxAB*. *Gene* **150**, 169–174 (1994).
35. Contag, C.H. *et al.* Photonic detection of bacterial pathogens in living hosts. *Mol. Microbiol.* **18**, 593–603 (1995).
36. Shabahang, S. & Szalay, A.A. in *Proceedings of the 11th International Symposium on Bioluminescence and Chemiluminescence, Pacific Grove, CA, September 6–10, 2000* (eds. Case, J.F. *et al.*) 449–452 (World Scientific, Singapore, 2001).
37. Wang, Y., Wang, G., O'Kane, D.J. & Szalay, A.A. in *Proceedings of the 9th International Symposium on Bioluminescence and Chemiluminescence, Woods Hole, MA, October 4–8, 1996* (eds. Hastings, J.W. *et al.*) 419–422 (Wiley, Chichester, UK, 1996).
38. Wang, Y., Wang, G., O'Kane D.J. & Szalay A.A. Chemiluminescence energy transfer to study protein-protein interaction in living cells. *Mol. Gen. Genet.* **264**, 578–587 (2001).
39. Wang, Y, Yu Y., Shabahang, S., Wang, G. & Szalay, A.A. Functional *Renilla* luciferase–*Aequorea* GFP (RUC-GFP) fusion protein as a novel dual reporter for imaging of gene expression in cell cultures and in live animals. *Mol. Gen. Genet.* **268**, 160–168 (2002).
40. Timiryasova, T., Yu, Y.A., Shabahang, S., Fodor, I. & Szalay, A.A. in *Proceedings of the 11th International Symposium on Bioluminescence and Chemiluminescence, Pacific Grove, CA, September 6–10, 2000* (eds. Case, J.F. *et al.*) 457–460 (World Scientific, Singapore, 2001).
41. Gebauer, G., Jager, W. & Lang, N. mRNA expression of components of the insulin-like growth factor system in breast cancer cell lines, tissues, and metastatic breast cancer cells. *Anticancer Res.* **18**, 1191–1195 (1998).
42. Padera, T.P. *et al.* Lymphatic metastasis in the absence of functional intratumor lymphatics. *Science* **296**, 1883–1886 (2002).
43. Mose, J.R. & Mose, G. Oncolysis by *Clostridia*. I. Activity of *Clostridium butyricum* (M-55) and other nonpathogenic *Clostridia* against the Ehrlich carcinoma. *Cancer Res.* **24**, 212–216 (1964).
44. Dang, L.H., Bettegowda, C., Huso, D.L., Kinzler, K.W. & Vogelstein, B. Combination bacteriolytic therapy for the treatment of experimental tumors. *Proc. Natl. Acad. Sci. USA* **98**, 15155–15160 (2001).
45. Yazawa, K., Fujimori, M., Amano, J., Kano, Y. & Taniguchi, S. *Bifidobacterium longum* as a delivery system for cancer gene therapy: selective localization and growth in hypoxic tumors. *Cancer Gene Ther.* **7**, 269–274 (2000).
46. Sznol, M., Lin, S.L., Bermudes, D., Zheng, L.M. & King, I. Use of preferentially replicating bacteria for the treatment of cancer. *J. Clin. Invest.* **105**, 1027–1030 (2000).
47. Ramshaw, I., Ruby, J., Ramsay, A., Ada, G. & Karupiah, G. Expression of cytokines by recombinant vaccinia virus: a model for studying cytokines in virus infections *in vivo*. *Immun. Rev.* **127**, 157–182 (1992).
48. Gnant, M.F.X., Puhlmann, M., Alexander H.R. & Bartlett, D.L. Systemic administration of a recombinant vaccinia virus expressing the cytosine deaminase gene and subsequent treatment with 5-fluorocytosine leads to tumor-specific gene expression and prolongation of survival in mice. *Cancer Res.* **59**, 3396–3403 (1999).
49. Voisey, C.R. & Marincs, F. Elimination of internal restriction enzyme sites from a bacterial luminescence (*luxCDABE*) operon. *Biotechniques* **24**, 56–58 (1998).

Science **227**, 1345–1347 (1985).

Erratum: Drugs in crops—the unpalatable truth

Editorial
Nat. Biotechnol. 22, 133 (2004)

On line 16 of the editorial, both Samyang Genex (Daejeon, Korea) and Maxygen (Redwood City, CA, USA) were wrongly indicated to be exploring the expression of biopharmaceuticals in corn. This erroneous information was obtained from a report *A Strategic Evaluation of Transgenic Plant and Animal Biomanufacturing Systems* (Revelogic, Ft. Collins, CO, USA, 2003). In fact, Samyang Genex has a corn processing plant and uses plant cell culture to produce paclitaxel, whereas Maxygen has no program focus on expressing biopharmaceuticals in corn.

Erratum: Make or break for costimulatory blockers

Ken Garber
Nat. Biotechnol. 22, 145–147 (2004)

In Box 1 on p. 147, column 1, line 13, the sentence "Antigen-presenting cell (APC) B7 signaling induces T cells to express the enzyme indoleamine 2,3 dioxygenase (IDO), which catabolizes the amino acid tryptophan, presumably starving T cells and causing proliferation arrest" should have read, "B7 signaling in antigen-presenting cells (APCs) leads them to express the enzyme indoleamine 2,3 dioxygenase (IDO), which catabolizes the amino acid tryptophan, presumably starving T cells and causing proliferation arrest."

Corrigendum: Visualization of tumors and metastases in live animals with bacteria and vaccinia virus encoding light-emitting proteins

Yong A Yu, Shahrokh Shabahang, Tatyana M Timiryasova, Qian Zhang, Richard Beltz, Ivaylo Gentschev, Werner Goebel & Aladar A Szalay
Nat. Biotechnol. 22, 313–320 (2003)

On page 319, column 1, line 9 from bottom, the phrase "subcutaneous colon fibrosarcoma" should have read "subcutaneous fibrosarcoma."

Corrigendum: Phenotypic alteration of eukaryotic cells using randomized libraries of artificial transcription factors

Kyung-Soon Park[1,2], Dong-ki Lee[1,2], Horim Lee[1], Yangsoon Lee[1], Young-Soon Jang[1], Yong Ha Kim[1], Hyo-Young Yang[1], Sung-Il Lee[1], Wongi Seol[1] & Jin-Soo Kim[1]
Nat. Biotechnol. 21, 1208–1214 (2003)

In the author list, the name of author Seong-il Lee was misspelled as Sung-Il Lee.